AMERICAN SOCIETY FOR MICROBIOLOGY | mBio®

RESEARCH ARTICLE

Widespread Distribution and Functional Specificity of the Copper Importer CcoA: Distinct Cu Uptake Routes for Bacterial Cytochrome *c* Oxidases

Bahia Khalfaoui-Hassani,[a]* Hongjiang Wu,[a] Crysten E. Blaby-Haas,[b] Yang Zhang,[a] Federica Sandri,[a] Andreia F. Verissimo,[a] Hans-Georg Koch,[c] Fevzi Daldal[a]

[a]Department of Biology, University of Pennsylvania, Philadelphia, Pennsylvania, USA

[b]Biology Department, Brookhaven National Laboratory, Upton, New York, USA

[c]Institut für Biochemie und Molekularbiologie, ZMBZ, Faculty of Medicine, Albert-Ludwigs-Universität, Freiburg, Germany

ABSTRACT Cytochrome *c* oxidases are members of the heme-copper oxidase superfamily. These enzymes have different subunits, cofactors, and primary electron acceptors, yet they all contain identical heme-copper (Cu_B) binuclear centers within their catalytic subunits. The uptake and delivery pathways of the Cu_B atom incorporated into this active site, where oxygen is reduced to water, are not well understood. Our previous work with the facultative phototrophic bacterium *Rhodobacter capsulatus* indicated that the copper atom needed for the Cu_B site of cbb_3-type cytochrome *c* oxidase (cbb_3-Cox) is imported to the cytoplasm by a major facilitator superfamily-type transporter, CcoA. In this study, a comparative genomic analysis of CcoA orthologs in alphaproteobacterial genomes showed that CcoA is widespread among organisms and frequently co-occurs with cytochrome *c* oxidases. To define the specificity of CcoA activity, we investigated its function in *Rhodobacter sphaeroides*, a close relative of *R. capsulatus* that contains both cbb_3- and aa_3-Cox. Phenotypic, genetic, and biochemical characterization of mutants lacking CcoA showed that in its absence, or even in the presence of its bypass suppressors, only the production of cbb_3-Cox and not that of aa_3-Cox was affected. We therefore concluded that CcoA is dedicated solely to cbb_3-Cox biogenesis, establishing that distinct copper uptake systems provide the Cu_B atoms to the catalytic sites of these two similar cytochrome *c* oxidases. These findings illustrate the large variety of strategies that organisms employ to ensure homeostasis and fine control of copper trafficking and delivery to the target cuproproteins under different physiological conditions.

IMPORTANCE The cbb_3- and aa_3-type cytochrome *c* oxidases belong to the widespread heme-copper oxidase superfamily. They are membrane-integral cuproproteins that catalyze oxygen reduction to water under hypoxic and normoxic growth conditions. These enzymes diverge in terms of subunit and cofactor composition, yet they all share a conserved heme-copper binuclear site within their catalytic subunit. In this study, we show that the copper atoms of the catalytic center of two similar cytochrome *c* oxidases from this superfamily are provided by different copper uptake systems during their biogenesis. This finding illustrates different strategies by which organisms fine-tune the trafficking of copper, which is an essential but toxic micronutrient.

KEYWORDS CcoA, cytochrome, copper homeostasis, copper transport, copper uptake, cytochrome biogenesis, cytochrome *c* oxidase

Copper (Cu) is an important micronutrient required for the survival of virtually all living organisms, as numerous cellular processes depend on cuproproteins (1, 2). At high concentrations, Cu is extremely toxic for cells and can cause severe oxidative

Received 12 January 2018 **Accepted** 19 January 2018 **Published** 27 February 2018

Citation Khalfaoui-Hassani B, Wu H, Blaby-Haas CE, Zhang Y, Sandri F, Verissimo AF, Koch H-G, Daldal F. 2018. Widespread distribution and functional specificity of the copper importer CcoA: distinct Cu uptake routes for bacterial cytochrome *c* oxidases. mBio 9:e00065-18. https://doi.org/10.1128/mBio.00065-18.

Editor Howard A. Shuman, University of Chicago

Address correspondence to Fevzi Daldal, fdaldal@sas.upenn.edu.

* Present address: Bahia Khalfaoui-Hassani, Equipe Microbiologie et Environement (Bâtiment IBEAS), IPREM, UMR CNRS 5254, Université de Pau et des Pays de l'Andour, Pau, France.

B.K.-H. and H.W. contributed equally to this work.

This article is a direct contribution from a Fellow of the American Academy of Microbiology. Solicited external reviewers: J. Thomas Beatty, University of British Columbia; David Giedroc, Indiana University Bloomington; Jonathan Hosler, University of Mississippi Medical Center.

damage by competing with other divalent metal cations (e.g., iron) or by triggering the Fenton reaction (3, 4). Indeed, both Cu deficiency and excess cause serious human disorders, including Menkes, Wilson's, and Alzheimer's diseases (5–7). Therefore, Cu homeostasis is crucial for organisms, and cells tightly control their Cu content, from its uptake to its incorporation into cuproproteins (8, 9).

Heme-copper oxidases (HCOs) are major Cu-containing enzymes located in the cytoplasmic membranes of bacteria and archaea and in the mitochondrial inner membranes (10, 11). They are widespread among all domains of life as key components of the respiratory electron transport chain, catalyzing the reduction of oxygen to water while pumping protons across the membrane. HCOs are classified in three major families (A, B, and C) based on conserved residues forming the proton pathways within their catalytic subunit I (12). Although they differ in the number of subunits and cofactor composition, they all contain a conserved catalytic subunit carrying a low-spin heme and a heterobinuclear metal center composed of a Cu atom (referred to as Cu_B) and a high-spin heme. The type A aa_3-type cytochrome (cyt) *c* oxidases (aa_3-Cox) are present in mitochondria and widespread in bacteria and archaea (13, 14). Two of the subunits of aa_3-Cox harbor all of the cofactors required for catalysis. Subunit I (Cox1) is the conserved membrane integral catalytic subunit, which contains a low-spin heme *a* and a heterobinuclear center composed of a high-spin heme *a* (heme a_3) and a Cu_B atom. Subunit II (Cox2) contains a homobinuclear Cu center (Cu_A) that receives electrons from a cyt *c* donor. Depending on the species, the aa_3-Cox enzymes may contain additional subunits with no cofactors. Biogenesis of the Cu centers of mitochondrial aa_3-Cox requires plasma membrane-integral Cu transporters (known as Ctr) that import Cu into the cytoplasm and multiple chaperones (11, 15, 16). In yeast mitochondria, Cu is imported into the mitochondrial matrix before being inserted into aa_3-Cox (17). The Cu chaperone Cox17 conveys the Cu in the mitochondrial intermembrane space to Sco1/Sco2 proteins for incorporation into the Cu_A center in Cox2 or to Cox11 for assembly of the Cu_B center in Cox1 subunits, respectively (18–21). In bacteria, periplasmic chaperones (e.g., PCu_AC-like [22]) act as functional homologues of mitochondrial Cox17 and, together with the homologues of Sco1/Sco2 (SenC [23] or PrrC [24]), deliver Cu to the Cu_A center of aa_3-Cox (22). Similarly, Cox11 homologues are required for the insertion of Cu_B into bacterial aa_3-Cox, but its source of Cu remains unknown (24, 25).

Class C HCOs are cbb_3-type cyt *c* oxidases (cbb_3-Cox) that are found only in bacteria (26). They are the most divergent type of HCO and differ from class A aa_3-Cox by containing three functional subunits (instead of two) and different cofactors (27). CcoN (subunit I) is the main catalytic subunit, which is the functional analogue of Cox1. It is an integral membrane protein and contains a low-spin heme *b* and a heterobinuclear center composed of a high-spin heme *b* (heme b_3) coupled to the Cu_B atom. cbb_3-Cox has no structural homologue of Cox2 or Cu_A center (27). Instead, it contains a dihemic cyt *c* subunit (CcoP), acting as the primary electron acceptor of cbb_3-Cox. CcoP transfers the electrons via the monohemic cyt *c* subunit (CcoO) to the low-spin heme *b* and finally to the binuclear center heme b_3-Cu_B of the CcoN subunit (13, 28). Cu_B atom incorporation into CcoN requires several transporters and chaperones (27). The P_{1B}-type ATPase CcoI (29) (also known as CopA2 [30] or CtpA [31]), which is similar to the Cu-detoxifying transporter CopA (32) (or CopA1 [30]), is a Cu exporter located in the cytoplasmic membrane and is required for cbb_3-Cox biogenesis. The fate of the Cu exported by CcoI is currently unclear. Possibly, it can be delivered either directly to the catalytic center of CcoN or to other periplasmic Cu chaperones. At low Cu availability, the Cu chaperones SenC (in *R. capsulatus* [23]) and PrrC (in *R. sphaeroides* [24]), which are homologues of mitochondrial Sco1/Sco2, and their interacting partners PccA (of *R. capsulatus* [33]) and PCu_AC (of *R. sphaeroides* [24]) are needed for cbb_3-Cox biogenesis. Finally, a member of the major facilitator superfamily (MFS) of transporters, CcoA, is a Cu importer that is required for assembly of the Cu_B center of cbb_3-Cox (32, 34, 35). *R. capsulatus* mutants lacking CcoA are impaired for Cu uptake and contain a very small amount of cbb_3-Cox (34). This importer is the first MFS member involved in metal transport and defines a new family of "copper uptake porters" (2.A.1.81) among the

MFS-type transporters (http://www.tcdb.org/) (36). Recent studies showed that conserved Met and His residues of CcoA are important for its function, possibly acting as metal ligands (37). It is noteworthy that both the Cu importer CcoA and the Cu exporter CcoI are required to incorporate the Cu_B center into CcoN, implying trafficking of Cu across the cytoplasmic membrane during cbb_3-Cox biogenesis (32).

In this study, we conducted comparative genomic analyses of CcoA orthologs in alphaproteobacterial genomes. This search revealed a higher degree of co-occurrence of CcoA with cbb_3-Cox than with aa_3-Cox, suggesting that CcoA activity is specific to class C HCOs. To test this hypothesis, we investigated the function of CcoA in *R. sphaeroides*, a close relative of *R. capsulatus*, which contains both functional cbb_3- and aa_3-Cox with identical heme-Cu_B binuclear centers, belonging to different HCO families. Upon the identification of *R. sphaeroides ccoA* (RSP_2726), appropriate mutants were constructed and their physiological and biochemical properties were characterized. We also identified bypass suppressors of Δ*ccoA* mutants in *R. sphaeroides copA* (RSP_2890) that restored cbb_3-Cox activity at the expense of increased Cu^{2+} sensitivity. This study showed that CcoA is specific to cbb_3-Cox and is not involved in the biogenesis of aa_3-Cox. Therefore, we concluded that the Cu atoms needed for the formation of the heme-Cu_B binuclear centers in these two similar enzymes must be provided by distinct Cu uptake pathways.

RESULTS

Distribution of CcoA homologues in alphaproteobacteria. Using CcoA from *R. capsulatus* as a query, we identified 144 CcoA-like MFS proteins in 125 of the 327 alphaproteobacterial species interrogated, with several genomes containing up to three distinct copies of *ccoA*. We also compiled a phylogenetic profile of *ccoA* together with the presence of the cbb_3-Cox and aa_3-Cox structural genes (Fig. 1A). Most of the CcoA homologues were predicted to contain 12 transmembrane helices with conservation of the motifs MXXXM in helix 7 and HXXXM in helix 8, both of which are required for Cu uptake and for cbb_3-Cox activity in *R. capsulatus* (37), with the exception of a group of CcoA-like proteins in *Rhizobiales* (Fig. 1B). These putative transporters also contained the two conserved motifs in helices 7 and 8 but were truncated at the C terminus, lacking predicted helix 12. Intriguingly, the genes encoding these truncated CcoA homologues were found right downstream of the *ccoNOQP* and *ccoGHIS* clusters, encoding the structural and assembly genes of cbb_3-Cox, respectively (Fig. 1B), suggesting that the *Rhizobiales* CcoA-like proteins might play a role similar to that of *R. capsulatus* CcoA. For the complete set of data pertinent to Fig. 1, see Table S1 in the supplemental material.

We found that of the 327 alphaproteobacterial genomes analyzed, only 44 had no CcoA or Cox enzyme (Fig. 2; Table S2). Among the remaining genomes, 118 (62%) of 192 coding for cbb_3-Cox (CcoNOQP) and 122 (46%) of 274 coding for aa_3-Cox (CoxI, CoxII, and CoxIII) also contained CcoA. In contrast, 74 (23%) of these genomes had cbb_3-Cox but not CcoA (mainly from *Caulobacterales*, *Brucella*, *Rhizobiaceae*, *Hyphomonadaceae*, *Rhodospirillaceae*, and *Sphingomonadales*), while 152 (46%) had aa_3-Cox without CcoA (Fig. 2; Table S2). Thus, the data suggested a higher degree of co-occurrence of *ccoA* and cbb_3-Cox than of *ccoA* and aa_3-Cox. This co-occurrence was particularly evident in *Methylocystaceae* and *Methylobacteriaceae*, where species of the same genus would have both CcoA and cbb_3-Cox or neither (Fig. 1C). In addition, we also observed strain differences; e.g., both *Paracoccus denitrificans* strains SD1 and PD1222 had cbb_3-Cox and aa_3-Cox but only strain PD1222 contained CcoA. Similarly, all of the *Rhizobium leguminosarum* strains analyzed had cbb_3-Cox and aa_3-Cox but individual biovars differed in the presence of CcoA. Finally, we found six species containing cbb_3-Cox without CcoA and seven species containing CcoA but not cbb_3-Cox, suggesting that CcoA-independent provision of Cu to cbb_3-Cox and an additional unknown function(s) of CcoA, that is unrelated to Cu provision to the Cu_B center of this enzyme might exist in some species (Table S2).

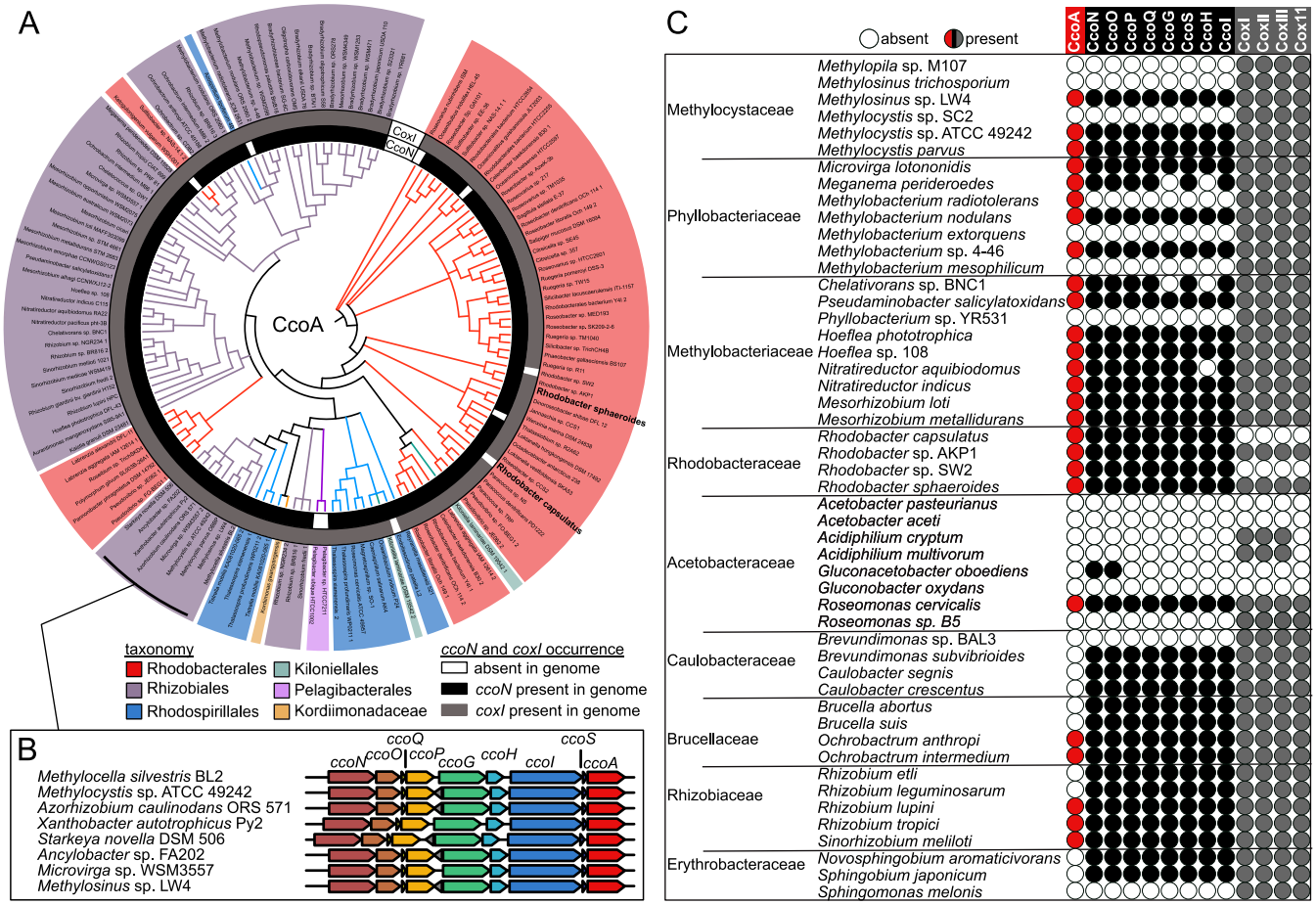

FIG 1 Presence of CcoA homologues encoded in alphaproteobacterial genomes. (A) Evolutionary relationships between the CcoA homologues identified in sequenced alphaproteobacterial genomes. Branch lengths were ignored, and branch points with Shimodaira-Hasegawa scores of <0.5 were deleted. Branches and nodes are colored by order as shown at the bottom of panel A. The presence of *ccoN* (inner circle) or *cox1* (outer circle) in each genome is represented by black or gray shading, respectively. Corresponding protein IDs are listed in Table S1. (B) Schematic representation of the cbb_3-Cox structural (*ccoNOQP*) and assembly (*ccoGHIS*) gene clusters together with the *ccoA* homologue in the *Rhizobiales* genomes indicated. (C) Co-occurrence plot with circles indicating the presence or absence of *ccoA* (red or white, respectively), the cbb_3-Cox structural and assembly gene clusters (black or white, respectively), and the aa_3-Cox-related genes (gray or white, respectively). Not all species are shown because of space limitations, but for a complete profile and a summary, see Tables S1 and S2, respectively.

Phenotypes of *ccoA* mutants of *R. sphaeroides*. To understand the role of CcoA in the biogenesis of the Cu_B site of HCO and to test whether CcoA is involved in the provision of Cu to aa_3-Cox, as it is in the provision of Cu to cbb_3-Cox, we investigated the function of a CcoA ortholog in an organism that contains multiple HCOs. *R. sphaeroides* has a CcoA homologue (RSP_2726, previously annotated as a multidrug/metabolite efflux pump) containing the conserved Met motifs in transmembrane helices 7 and 8 (Fig. 3A). Unlike *R. capsulatus*, which is rare among the alphaproteobacterial species in having only one HCO (cbb_3-Cox), *R. sphaeroides* also contains the canonical type A aa_3-Cox. To assess the effect of lacking CcoA on both cbb_3- and aa_3-Cox activities, a *ccoA* deletion allele was introduced into appropriate *R. sphaeroides* strains. The wild-type (Ga) strain and the Δaa_3 (JS100 [38]) and Δcbb_3 (MT001 [39, 40]) mutant strains yielded the Δ*ccoA* (HW3) single mutant and the Δ*ccoA* Δaa_3 (HW2) and Δ*ccoA* Δcbb_3 (HW4) double mutants, respectively (Table S3). The Δcbb_3 Δaa_3 double mutant (ME127 [40]), lacking both cbb_3- and aa_3-Cox activities, served as a negative control (Table S3). The Cox activities of these strains were visualized qualitatively by α-naphthol and *N*′*N*′-dimethyl-*p*-phenylenediamine (NADI; blue) staining of colonies grown aerobically on enriched medium (Fig. 3B). The wild-type and Δaa_3 mutant strains were $NADI^+$ (i.e., stained dark blue in seconds), whereas the Δcbb_3 mutant was

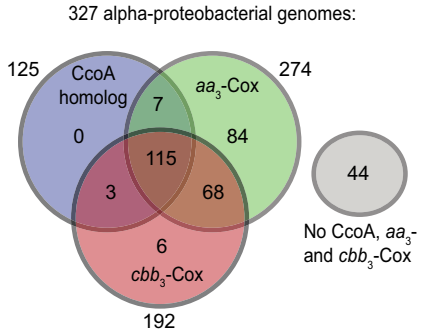

FIG 2 Distribution of CcoA, aa_3-Cox, and cbb_3-Cox homologues among the alphaproteobacterial genomes analyzed. Note that 44 genomes have no CcoA, aa_3-Cox, or cbb_3-Cox homologues, whereas 115 have all of them. Of the genomes that have no CcoA, 68 have both aa_3-Cox or cbb_3-Cox, while 84 have only aa_3-Cox and 6 have only cbb_3-Cox. Note that of the CcoA-containing genomes, only three have only cbb_3-Cox and seven have only aa_3-Cox.

NADI^{slow} (i.e., stained blue in a few minutes), indicating that cbb_3-Cox provides most of the Cox activity under these growth conditions. The Δaa_3 Δcbb_3 double mutant was NADI$^-$ (i.e., no blue staining after 15 min), consistent with the absence of both Cox enzymes (39). Both the Δ*ccoA* single mutant and the Δ*ccoA* Δcbb_3 double mutant had a NADI^{slow} phenotype, similar to that observed when only aa_3-Cox activity (Δcbb_3) was present (Fig. 3B). Importantly, the double mutant lacking both CcoA and aa_3-Cox (Δ*ccoA* Δaa_3) but containing the intact structural genes of cbb_3-Cox was NADI$^-$ like the double mutant (Δcbb_3 Δaa_3) lacking both Cox activities (Fig. 3B). Upon complementation with a plasmid carrying a wild-type allele of *R. sphaeroides ccoA*, both the single (Δ*ccoA*) and double (Δ*ccoA* Δaa_3) mutants lacking CcoA became NADI$^+$ (Fig. 3B). Thus, the data indicated that in *R. sphaeroides*, the absence of *ccoA* affected cbb_3-Cox, but not aa_3-Cox, activity.

The NADI$^-$ phenotypes of *R. sphaeroides* Δ*ccoA* mutants were restored upon the addition of 5 μM Cu^{2+} to the growth medium, similar to that seen in the *R. capsulatus* Δ*ccoA* mutant (34). In contrast, the Δ*ccoA* Δcbb_3 double mutant, which has only a functional aa_3-Cox, remained NADI^{slow} upon Cu^{2+} supplementation, suggesting that Cu^{2+} addition had no effect on aa_3-Cox activity (data not shown).

Absence of CcoA affects heme and subunit compositions of cbb_3-Cox but not aa_3-Cox. To assess how the absence of CcoA affects *R. sphaeroides* HCO biogenesis, the *c*-, *b*-, and *a*-type heme contents of membrane fractions derived from appropriate mutants were analyzed by using optical difference (dithionite-reduced minus ferricyanide-oxidized) spectra. In membranes of a wild-type *R. sphaeroides* strain, prominent peaks around 605, 560, and 551 nm, corresponding to the *a*-, *b*-, and *c*-type hemes, respectively, were readily detectable (39) (Fig. 3C). As expected, a significant decrease in the 605-nm peak and in the 560- and 551-nm peaks was observed in the Δaa_3 and Δcbb_3 mutants, respectively (41). Note that in *R. sphaeroides* membranes, only aa_3-Cox has *a*-type heme but other proteins besides cbb_3-Cox contain *b*- and *c*-type hemes (e.g., cyt bc_1) under the growth conditions tested. Accordingly, in the double mutant (Δcbb_3 Δaa_3) lacking both Cox enzymes, all three peaks decreased substantially compared with the wild-type strain (Fig. 3C), as reported earlier (39). Remarkably, in the Δ*ccoA* single mutant only the content of *b*- and *c*-type hemes decreased, as in the mutant lacking only cbb_3-Cox (Δcbb_3) or the Δ*ccoA* Δcbb_3 double mutant. Moreover, in the Δ*ccoA* Δaa_3 double mutant, all three peaks, corresponding to the *a*-, *b*-, and *c*-type hemes, decreased drastically, similar to what was seen in the double mutant (Δcbb_3 Δaa_3) (Fig. 3C). In summary, the data showed that in the absence of CcoA, the content of *b*- and *c*-type hemes in the membrane fraction (corresponding partly to cbb_3-Cox) decreased significantly, whereas the *a*-type heme content (corresponding to aa_3-Cox) remained unchanged, consistent with CcoA being involved in cbb_3-Cox, but not aa_3-Cox, production. We emphasize that these data are merely semiquantitative be-

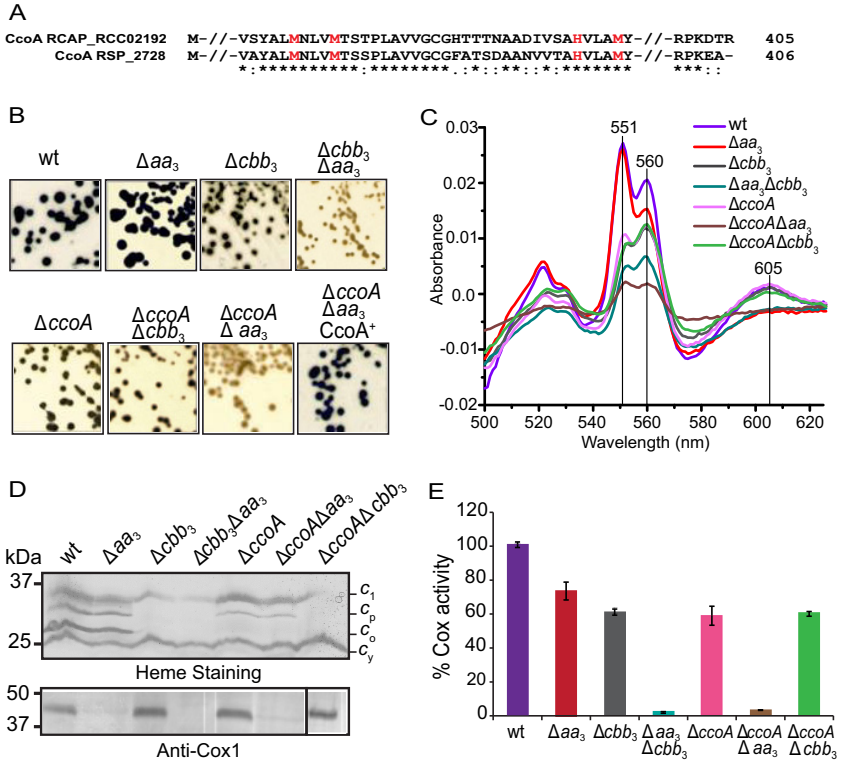

FIG 3 Met motifs of CcoA and phenotypic and functional characterization of *R. sphaeroides* Δ*ccoA* mutants. (A) Amino acid sequence alignment of the highly conserved region surrounding the Met and His motifs MXXXM and HXXXM (in red) from *R. capsulatus* CcoA (RCA_RCC02192) and its *R. sphaeroides* homologue (RSP_2726) (65% identity; 80% similarity). (B) Growth and NADI phenotypes of colonies of *R. sphaeroides* wild-type (wt) Ga and Δaa_3 (JS100), Δcbb_3 (MT001), and Δaa_3 Δcbb_3 (ME127) Cox mutants together with those of Δ*ccoA* (HW3), Δ*ccoA* Δcbb_3 (HW24), and Δ*ccoA* Δaa_3 (HW2) CcoA mutants. Cells were grown aerobically at 35°C on LB medium, and the presence of Cox activity was visualized by NADI staining (see Materials and Methods). Colonies that contain wild-type levels of Cox activity turn dark blue within a few seconds ($NADI^+$), while those that have low or no Cox activity show lighter blue ($NADI^{slow}$) or no blue staining ($NADI^-$) upon longer exposure, respectively. Note that the Δ*ccoA* Δaa_3 mutant is $NADI^-$ like the Δaa_3 Δcbb_3 mutant, unless it is complemented with a plasmid carrying a wild-type allele of *ccoA* (Δ*ccoA* Δaa_3 $CcoA^+$). (C) Absorption difference spectra of membrane fractions of *R. sphaeroides* mutants recorded between 500 and 625 nm by using oxidized membrane preparations as the baseline and reducing the sample with an excess of sodium dithionite. The intensity of the peaks centered at 551, 560, and 605 nm indicates the contents of *c*-, *b*- and *a*-type hemes, respectively. (D) Steady-state levels of structural subunits of cbb_3- and aa_3-Cox enzymes in the membranes of *R. sphaeroides* mutants. (Top) Membrane preparations of *R. sphaeroides* mutants separated by SDS-PAGE and then stained with TMBZ. Four different cyts *c* (cyt c_1 of the cyt bc_1 complex, cyt c_p [CcoP] and c_o [CcoO] subunits of cbb_3-Cox, and the membrane-attached electron carrier cyt c_y) can be seen in the wild-type strain (39). In the Δ*ccoA* mutant, the steady-state levels of cyt c_p and especially cyt c_o are very low. (Bottom) Membrane preparations of *R. sphaeroides* strains resolved by SDS-PAGE and subjected to immunoblot analysis. The presence of the Cox1 subunit of *R. sphaeroides* aa_3-Cox was identified with *P. denitrificans* Cox1 polyclonal antibodies that cross-react with it. The white lines seen on the blot next to some lanes are scanning artifacts and do not reflect spliced gels. (E) cyt *c* activity of membrane fractions of *R. sphaeroides* Δ*ccoA* mutants. Total Cox (cbb_3-Cox plus aa_3-Cox) activities were determined using membrane preparations of various *R. sphaeroides* strains by monitoring the rate of oxidation of reduced horse heart cyt *c*. *R. sphaeroides* wild-type strain Ga exhibited an activity of ~1.33 μmol of cyt *c* oxidized/min/mg of total membrane proteins, which was referred to as 100%. Three independent assays were carried out for each strain. The Δ*ccoA* Δaa_3 mutant has no activity, like the Δaa_3 Δcbb_3 mutant that lacks both Cox enzymes.

cause of the presence of other *b*- and *c*-type cyts (in addition to cbb_3-Cox) whose content may vary in the presence or absence of different HCOs.

Next, the steady-state amounts of cbb_3-Cox subunits present in membranes from appropriate mutants were examined by SDS-PAGE and 3,3′,5,5′-tetramethylbenzidine (TMBZ) staining, which specifically reveals membrane-bound *c*-type cyts (42). In wild-type *R. sphaeroides* membranes, four distinct *c*-type cyts, including the CcoO (cyt c_o) and CcoP (cyt c_p) subunits of cbb_3-Cox, can be detected (Fig. 3D, top). As expected, in

the absence of aa_3-Cox, the *c*-type cyt profile remained unchanged, but in mutants lacking cbb_3-Cox (Δ*cbb*$_3$ and Δ*cbb*$_3$ Δ*aa*$_3$), cyt c_o and cyt c_p were not present, leaving only the cyt c_1 subunit of cyt bc_1 and the membrane-anchored electron carrier cyt c_y. Remarkably, in strains lacking CcoA, such as the Δ*ccoA* and Δ*ccoA* Δ*aa*$_3$ mutants, the amounts of cyt c_o and cyt c_p decreased at different levels, even though these strains contained an intact copy of the cbb_3-Cox structural genes. These data, together with the spectral data showing that the amount of *b*-type heme, and hence that of CcoN, also decreased, indicated that production of cbb_3-Cox was defective in the absence of CcoA. Finally, the presence of the Cox1 subunit of aa_3-Cox was monitored by using polyclonal antibodies raised against Cox1 of *Paraccocus denitrificans* aa_3-Cox (43) (Fig. 3D, bottom). As expected, Cox1 was absent from mutants lacking aa_3-Cox, like the Δ*aa*$_3$, Δ*cbb*$_3$ Δ*aa*$_3$, and Δ*ccoA* Δ*aa*$_3$ mutant strains. However, it was readily detected in strains lacking CcoA (Δ*ccoA* mutant), cbb_3-Cox (Δ*cbb*$_3$ mutant), or both proteins (Δ*ccoA* Δ*cbb*$_3$ mutant) at levels comparable to those of the wild type, in agreement with the Cu-containing Cox1 subunit of aa_3-Cox being unaffected by the absence of CcoA in *R. sphaeroides*.

Cox activities of mutants lacking CcoA. The total cyt *c* oxidation activity (accounting for both aa_3-Cox and cbb_3-Cox activities) present in membranes of different *R. sphaeroides* strains was measured by using reduced horse heart cyt *c*. *R. sphaeroides* wild-type strain Ga exhibited an activity level of 1.33 μmol of cyt *c* oxidized/min/mg of total membrane proteins (referred to as 100%) (Fig. 3E). Addition of 200 μM KCN, a specific inhibitor of the HCO catalytic binuclear center, abolished this activity almost completely (96% inhibition). The mutants lacking aa_3-Cox (Δ*aa*$_3$ mutant) and cbb_3-Cox (Δ*cbb*$_3$ mutant) showed Cox activities corresponding to 73 and 62% of the wild-type level, respectively, whereas the Δ*cbb*$_3$ Δ*aa*$_3$ double mutant had no activity. A strain lacking only CcoA (Δ*ccoA* mutant) or both CcoA and cbb_3-Cox (Δ*ccoA* Δ*cbb*$_3$ mutant) showed similar amounts of Cox activity, 59 and 60% of the wild-type level, respectively. In contrast, a strain lacking both CcoA and aa_3-Cox (Δ*ccoA* Δ*aa*$_3$ mutant), although it contained intact cbb_3-Cox structural genes, had no Cox activity, similar to a Δ*cbb*$_3$ Δ*aa*$_3$ double mutant (Fig. 3E). Therefore, the absence of CcoA affected only cbb_3-Cox, and not aa_3-Cox, in *R. sphaeroides*.

Suppressors of Δ*ccoA* restore cbb_3-Cox activity at the expense of Cu^{2+} hypersensitivity. During the phenotypic characterization of Δ*ccoA* mutants, we observed that the $NADI^-$ double mutant lacking both CcoA and aa_3-Cox (Δ*ccoA* Δ*aa*$_3$ mutant) readily yielded wild-type-like $NADI^+$ revertants (Fig. 4A). Similar revertants had previously been obtained with *R. capsulatus* Δ*ccoA* mutants, and their characterization showed that these suppressor mutations restored cbb_3-Cox deficiency and conferred Cu^{2+} sensitivity (32). Using whole-genome sequencing, we determined that these mutations were single base-pair indels in a rare stretch of 10 conserved cytosine base pairs located in *copA*, which encoded the P_{1B}-type ATP-dependent Cu exporter (CopA) (32). These indels caused translational frameshifts that inactivated *copA* and increased cellular Cu content and Cu^{2+} sensitivity (32).

Intrigued by the occurrence of similar revertants of *R. sphaeroides*, we retained four independent $NADI^+$ derivatives ($HW2R_1$ to $HW2R_4$) of the Δ*ccoA* Δ*aa*$_3$ double mutant (Table S3) and tested their Cu^{2+} tolerance in enriched medium. Indeed, they were hypersensitive to Cu^{2+} (above ~200 μM) compared with their wild-type and Δ*ccoA* Δ*aa*$_3$ mutant parents (tolerant to ~1 mM) (Fig. 4B). Thus, similar to *R. capsulatus*, these *R. sphaeroides* revertants regained cbb_3-Cox activity at the expense of becoming hypersensitive to Cu^{2+}. DNA sequencing of the genomic copies of *R. sphaeroides copA* (RSP_2890) (44) from these revertants showed that they all contained two base-pair (CG) deletions in *copA* (Fig. 4C). Remarkably, these deletions were located in a region of *copA* containing five consecutive CG repeats, presumably causing translational frameshifts that inactivated *copA* and increased the Cu^{2+} sensitivity of cells. The data indicated that in *R. sphaeroides*, as in *R. capsulatus*, suppression of the CcoA defect

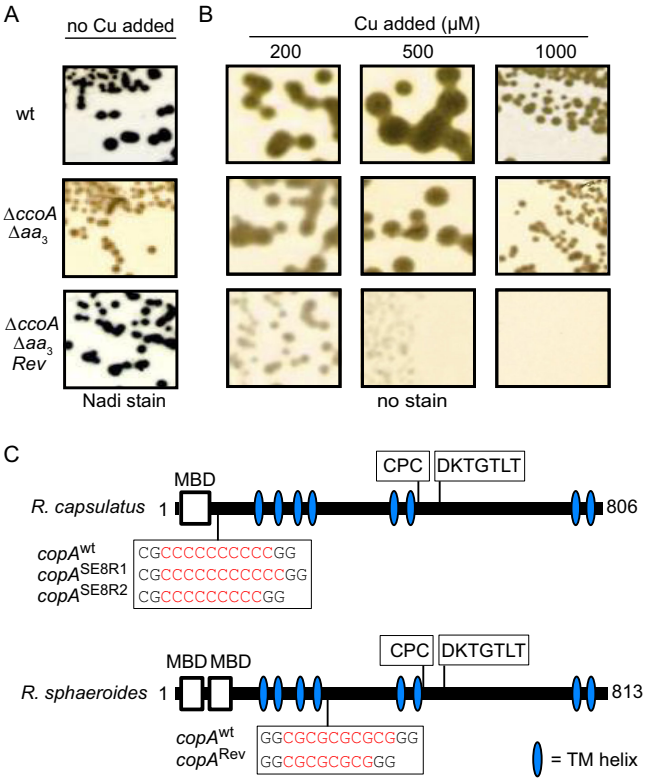

FIG 4 Bypass suppressors of *R. sphaeroides* mutants lacking CcoA are located in CopA and regain cbb_3-Cox activity at the expense of Cu^{2+} hypersensitivity. (A) Spontaneous $NADI^+$ bypass suppressors Δ*ccoA* Δaa_3/Rev_i that regained cbb_3-Cox activity were isolated from the Δ*ccoA* Δaa_3 mutant. (B) The Δ*ccoA* Δaa_3/Rev_i suppressors exhibit hypersensitivity to Cu^{2+} compared with the wild type (wt) and the Δ*ccoA* Δaa_3 mutant. (C) The suppressor mutations corresponded to 2-bp (CG) deletions in *copA* (RSP_2829) of *R. sphaeroides* in a stretch of five CG repeats located immediately after the fourth transmembrane segment. They are compared with similar CcoA suppressors ($CopA^{SE8R1}$ and $CopA^{SE8R2}$) isolated previously from *R. capsulatus* (32). The latter mutations corresponded to a single-base-pair (C) indel located in a stretch of 10 C repeats of *R. capsulatus* CopA before its first transmembrane helix. In both species, the suppressor mutations led to translational frameshifts that abolished CopA activity, leaving intact the possibility of producing N-terminally truncated polypeptides that still carry the MBDs. The N-terminal MBD, the phosphorylation domain (DKTGT), and the transmembrane metal binding motif (CPC) are represented in CopA.

occurred via mutations (two base-pair CG deletions and single base-pair C indels, respectively), inducing translational frameshifts that inactivated CopA.

Distribution of the CcoA family among *Bacteria* and *Eukarya*. Given the functional specificity of CcoA for cbb_3-Cox in *Rhodobacter* species, we widened our bioinformatic search for CcoA-like MFS transporters beyond the alphaproteobacteria and queried their co-occurrence with CcoN in the SEED database (45). We found CcoA homologues in all major classes of *Proteobacteria*, *Bacteroidetes*, and *Spirochaetia* and in all major divisions of the *Terrabacteria* group, including *Chloroflexi* and *Deinococcus* (Fig. 5A). Moreover, we found that most of the genomes that contained CcoA also encoded CcoN (i.e., cbb_3-Cox), except *Actinobacteria* and *Firmicutes* (Fig. 5B). The CcoA-like proteins were also present in the nuclear genomes of eukaryotic algae, with both primary and secondary plastids, in two fungal genomes from *Chytridiomycota* (Fig. 5A), in addition to the group of *Actinobacteria* and *Firmicutes* (Fig. 5B), which are known to lack cbb_3-Cox (26). Remarkably, these "orphan" CcoA-like transporters encountered in organisms lacking cbb_3-Cox still contained the conserved MXXXM and HXXXM motifs in helices 7 and 8, suggesting that they might also transport Cu to other protein targets. Finally, we note that, similar to alphaproteobacterial genomes, about one-third of *ccoN*-containing organisms also contain *ccoA* and exhibited species level

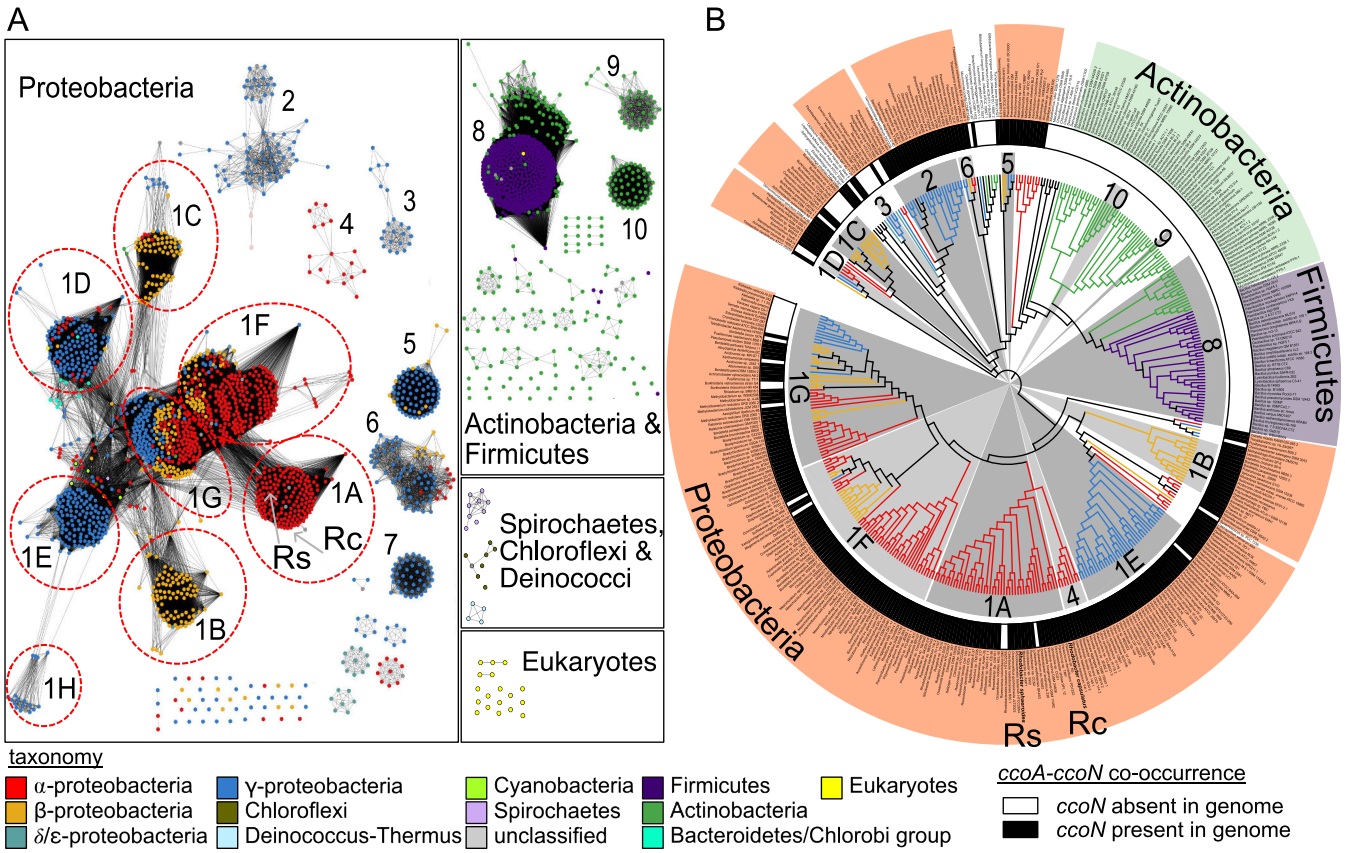

FIG 5 The CcoA-like family of putative transporters. (A) Protein similarity network of CcoA-like putative transporters identified in the Uniprot database. Each node (circle) represents a single protein sequence, and each edge (solid line) represents similarity between two proteins (threshold set at an alignment score of 80). Nodes are colored by taxonomy as shown at the bottom, and cluster designations (1 to 10) correspond to Table S4 and Fig. S1 PSN_CcoA.cys, which can be viewed in detail by using Cytoscape software. The locations of the nodes representing CcoA from *R. sphaeroides* (Rs) and *R. capsulatus* (Rc) are shown with gray arrows. (B) Evolutionary relationship between CcoA homologues identified in the SEED database. Branch lengths were ignored, and branch points with Shimodaira-Hasegawa scores of <0.5 were deleted. Branches are colored by taxonomy as shown at the bottom. The presence of *ccoN* (inner circle) in each genome is represented by black shading. Gray shading is used to color those clades that correspond to the numbered clusters (1A to 10) shown in panel A. Corresponding protein IDs are listed in Table S5. The positions of CcoA of *R. sphaeroides* (Rs) and *R. capsulatus* (Rc) in the tree are also indicated. Note that *ccoA* is present in *Actinobacteria* and *Firmicutes* (clusters 8 to 10) that are devoid of *ccoN* (i.e., cbb_3-Cox).

variation in its presence, which is particularly evident in *Vibrio* (Table S4). For the set of data pertinent to Fig. 5A and B, see Tables S4 and S5, respectively.

DISCUSSION

The *R. capsulatus* MFS-type transporter CcoA is the prototypical bacterial Cu importer and the key Cu provider to cbb_3-Cox under limited Cu availability (32, 34, 37). Earlier, we observed that *R. capsulatus* mutants lacking either cbb_3-Cox (Δ*ccoNOQP*) or CcoA (Δ*ccoA*) contained similar smaller amounts of total cellular Cu (~80% of the wild-type amount) (46), suggesting that the Cu imported by CcoA is allocated primarily to cbb_3-Cox biogenesis. To assess the functional specificity of CcoA toward other cuproenzymes, we initiated a broad-based comparative genomic study to examine the presence of CcoA homologues and their co-occurrence with cyt *c* oxidases in organisms of known genome sequences. We found that the CcoA-like transporters are widespread in bacteria and some microbial eukaryotes. They are present in all major classes of *Proteobacteria*, *Bacteroidetes*, *Spirochaetia*, and *Terrabacteria*, as well as in the nuclear genomes of eukaryotic algae and fungi (Table S1). Interestingly, our all-inclusive bioinformatic analyses showed that not all CcoA family members are involved in cbb_3-Cox biogenesis. Numerous species that have no cbb_3-Cox, such as *Actinobacteria* and *Firmicutes* species, still contained CcoA-like transporters that possibly perform other functions that have yet to be uncovered. A closer look to the group of alpha-

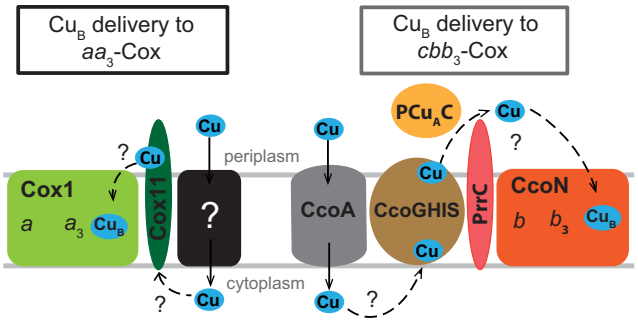

FIG 6 Schematic comparison of Cu_B incorporation into the active sites of bacterial aa_3- and cbb_3-Cox. A complete understanding of the pathways of Cu uptake and delivery to the heme-Cu_B binuclear site of HCOs is still missing. All known components involved in the biogenesis of the Cu_B center of bacterial aa_3- and cbb_3-Cox are depicted. In the case of aa_3-Cox, the Cox1 subunit is thought to receive Cu_B from the Cu chaperone Cox11 either directly or via an unknown partner(s). How Cu is initially conveyed to Cox11 remains unknown. A putative Cu importer of unknown identity (black box) that is possibly functionally similar to mitochondrial Pic2 (71) is included. In the case of cbb_3-Cox, Cu is imported by CcoA and is conveyed by the CcoGHIS, PCuAC, and PrrC (PccA and SenC homologs) assembly components to the Cu_B site of the CcoN subunit by a mechanism that remains elusive. Question marks indicate unknown Cu transfer steps.

proteobacteria showed that about one-third of these species contained at least one CcoA homologue together with the genes encoding cbb_3-Cox or aa_3-Cox, showing a high degree of co-occurrence of HCO with CcoA. Finally, similar to some genera of alphaproteobacteria, we observed species level variations in the presence of *ccoA*, which were particularly evident in *Vibrio* (Table S4), which may reflect that CcoA provides a selective advantage in some environmental niches.

Using *R. sphaeroides*, which contains both cbb_3- and aa_3-Cox (from C and A HCO families, respectively) and an ortholog of *R. capsulatus* CcoA (RSP_2726), we tested experimentally whether CcoA could also provide Cu to the canonical aa_3-Cox, whose biogenesis has been studied (43, 47). Physiological, genetic, and biochemical data gathered by using appropriate Δ*ccoA* mutants lacking either cbb_3- or aa_3-Cox established unequivocally that the absence of CcoA affected cbb_3-Cox, but not aa_3-Cox, production in this organism. Earlier work had shown that the absence of the Cu chaperone Cox11, which is required for Cu_B insertion into aa_3-Cox, had no effect on cbb_3-Cox production in *R. sphaeroides* (25) or *Pseudomonas pseudoalcaligenes* KF707 (48). Therefore, we concluded that the Cu atoms inserted into the binuclear centers of the cbb_3-Cox and aa_3-Cox enzymes are not only delivered by distinct pathways but also provided by different uptake systems (Fig. 6).

CcoA being an exclusive Cu importer for cbb_3-Cox was rather unexpected, especially because the catalytic subunits and the heme-Cu binuclear centers of all HCOs are very similar (11, 49). The existence of specialized Cu trafficking pathways for different cuproproteins has been documented in different organisms (50), and their specificity is generally conferred by target-specific chaperones rather than transporters (51). Thus, the independent Cu uptake systems operating during the biogenesis of different HCOs and the specificity of CcoA for cbb_3-Cox are intriguing. Since the Sco-like and PCu_AC-like Cu chaperones are involved in the biogenesis of both cbb_3-Cox (23, 27, 33) and aa_3-Cox (19, 22, 24, 52), they are less likely to confer specificity. Thus, a possibility is that CcoA may do so by conveying Cu either directly or via an unknown partner, to CcoI, which is the P_{1B}-type ATPase required for cbb_3-Cox production (29) (Fig. 6). Interestingly, the physical clustering of *ccoA* with the cbb_3-Cox assembly genes *ccoGHIS* in members of the order *Rhizobiales* (Fig. 1B) suggests that these proteins function together and possibly interact during cbb_3-Cox production. Undoubtedly, under low Cu availability, the occurrence of a membrane-integral complex containing both CcoI and CcoA would be advantageous for efficient biosynthesis of cbb_3-Cox.

In both *R. sphaeroides* and *R. capsulatus* mutants lacking CcoA, the defect in cbb_3-Cox production can be restored by providing a high concentration of exogenous

Cu^{2+}, which leads to an increase in cellular Cu content (34). The components of this putative CcoA-independent low-affinity Cu uptake pathway remain unknown. However, this pathway still relies on CcoI, whose absence cannot be palliated by Cu^{2+} supplementation, to provide Cu to cbb_3-Cox. Alternatively, the defect in cbb_3-Cox biogenesis can be bypassed via frameshift mutations in *copA*, which encodes the P_{1B}-type ATPase involved in Cu export and detoxification, resulting in inactivation of CopA and consequent greater cellular Cu content and hypersensitivity to Cu^{2+} (32). Elucidation of how the Cu imported by CcoA is conveyed to CcoI is needed to understand how the increase in cellular Cu content bypasses the role of CcoA in cbb_3-Cox biogenesis.

The molecular natures and locations of the suppressor mutations that inactivate CopA are different between the two *Rhodobacter* species. In *R. capsulatus*, these mutations are single base-pair C indels in a region of *copA* where 10 consecutive C base-pairs are located (bp 230 to 239) (32), whereas in *R. sphaeroides*, they are two base-pair CG deletions in a region of *copA* where five consecutive CG repeats are present (bp 863 to 872). Hypermutable nucleotide tandem repeats (NTRs), which are prone to DNA slippage during replication and increased recombination, are widespread in genomes of different organisms (53, 54), and they can reversibly inactivate or regulate the expression of specific coding sequences (55). Computational analyses suggested that in prokaryotes, the monomeric NTRs of G/C (e.g., C repeats of *R. capsulatus copA*) are more mutagenic than dimeric (e.g., CG repeats of *R. sphaeroides copA*) or trimeric NTRs (56). The different types of mutagenic NTRs located in *copA* may reflect different strategies used for Cu homeostasis governing Cu availability to cbb_3-Cox via CcoA-independent pathways.

P_{1B}-type ATPases such as CopA and CcoI contain conserved domains for ATP binding and for phosphorylation, in addition to their N-terminal metal-binding domains (MBDs), harboring a Cu-binding CXXC motif and a membrane-embedded Cu binding site (CPX) (57) (Fig. 4C). The frameshift mutations that inactivate CopA still conserve the genetic ability to produce truncated N-terminal CopA derivatives with intact N-terminal MBDs that, if produced and stable, could hypothetically facilitate Cu delivery to cbb_3-Cox. An *R. capsulatus* CopA derivative would become soluble with a single MBD, whereas an *R. sphaeroides* CopA derivative would remain membrane attached and conserve its two MBDs, reminiscent of the Cu chaperone CupA in *Streptococcus pneumoniae*. The membrane-anchored CupA protein enhances Cu sequestration and mediates its binding to the MBD of CopA as an adaptation to Cu toxicity (58). *Arabidopsis thaliana* chaperone PCH1 is produced by alternative splicing of the P_{1B}-type Cu^{+} ATPase PAA1 pre-mRNA and acts as its specific Cu chaperone (59). In *Escherichia coli*, a fragment of CopA containing the N-terminal MBD, resulting from programed ribosomal frameshifting during the translation of *copA* mRNA, is able to bind Cu and increase tolerance of Cu toxicity (60, 61). The molecular mechanisms underlying these cases are distinct from the NTR mutations in *copA*, yet they reflect similar responses that organisms have evolved to maintain Cu homeostasis and avoid its toxicity.

The isolation of mutations in *copA* of both *R. capsulatus* and *R. sphaeroides* may suggest that CcoA is not required for cbb_3-Cox metalation, depending on the mechanisms of Cu homeostasis used by the organisms. Indeed, our comparative genomic analyses indicated that CcoA-like MFS proteins are absent from about one-third of cbb_3-Cox-containing alphaproteobacterial species. That cbb_3-Cox metallation in these species does not require CcoA while it does so in *R. capsulatus* and *R. sphaeroides* under low Cu availability is intriguing. These species may have other Cu acquisition pathways, similar to *R. capsulatus ccoA* mutants at high Cu^{2+} concentrations. As an example, *P. denitrificans* PD1222 has an MFS-type CcoA Cu importer and a typical P_{1B}-type ATPase CopA ortholog with an N-terminal heavy-metal-associated (HMA) domain acting as its MBD. In contrast, *P. denitrificans* SD1 does not have CcoA but has a CopA homologue with a different MBD, an N-terminal TRASH domain (62). These differences are in agreement with the proposal that the *copA* NTR mutations occurring after the N-terminal MBD of CopA in both *Rhodobacter* species may result in HMA-containing

derivatives acting as chaperones. Further investigation of these species and characterization of different strains with respect to their CcoA-independent Cu trafficking pathways will be informative.

In summary, this work established that Cu incorporation into the catalytic site of different HCOs, in particular cbb_3-Cox and aa_3-Cox, occurs not only via distinct delivery pathways but also via distinct uptake pathways (Fig. 6). While the MFS-type transporter CcoA is required for Cu incorporation into cbb_3-Cox, it is not involved in the metallation of aa_3-Cox. The occurrence of dedicated Cu uptake pathways, critical for the maintenance of intracellular Cu homeostasis, might be an evolutionary example of different strategies to improve fitness encountered in many organisms.

MATERIALS AND METHODS

Bacterial strains, plasmids, and growth conditions. The *E. coli* and *R. sphaeroides* strains and plasmids used in this study are listed in Table S3. The standard molecular biology techniques used are described in reference 63, and all plasmid and strain constructions are described below Table S3. *E. coli* strains were grown at 37°C in Luria-Bertani (LB) broth supplemented with 100, 50, 50, 12.5, and 12 μg/ml (final concentrations) ampicillin, kanamycin (Kan), spectinomycin (Spe), tetracycline (Tet), and gentamicin (Gen), respectively (46). *R. sphaeroides* strains were grown in either minimal (64) or LB medium supplemented with 10, 10, 2.5, and 1 μg/ml (final concentrations) Kan, Spe, Tet, and Gen, respectively (39).

Biochemical and spectroscopic techniques. *R. sphaeroides* cells grown under semiaerobic conditions on LB medium were harvested and resuspended in 50 mM Tris-HCl (pH 7.2), 1 mM KCl assay buffer. Intracytoplasmic membrane vesicles (chromatophores) were prepared as previously described (65). The protein concentration of membrane fractions was determined with the bicinchoninic acid assay (Sigma, Inc.). Visualization of *c*-type cyts was done by TMBZ staining following the separation of ~200 μg of total membrane proteins by 15% SDS-PAGE as done earlier (42). Immunoblot analysis to identify *R. sphaeroides* Cox1 was done with ~40 μg of total membrane proteins separated by 12% SDS-PAGE. Proteins were transferred onto polyvinylidene difluoride membranes and incubated with *P. denitrificans* anti-Cox1 specific polyclonal antibodies cross-reacting with *R. sphaeroides* protein (47). Alkaline phosphatase-conjugated secondary antibodies and 5-bromo-4-chloro-3-indolyl phosphate (BCIP)–nitroblue tetrazolium were used for visualization of Cox1 polypeptide.

Visible spectra were taken with 50 μg of total membrane proteins in 1 ml of assay buffer containing 0.2% *n*-dodecyl-β-D-maltoside (DDM). Samples were oxidized by the addition of a few grains of potassium ferricyanide, and the absorption spectra taken between 480 and 660 nm were saved as a baseline. After reduction of the samples by the addition of a small amount of sodium dithionite, the spectra were rerecorded in the same wavelength range (39).

Determination of Cox activities. The cbb_3-Cox activity of colonies was visualized by using the NADI reaction (α-naphthol + *N*′*N*′-dimethyl-*p*-phenylenediamine $\rightarrow$ indophenol blue + H_2O) by staining the plates with a 1:1 (vol/vol) mixture of 35 mM α-naphthol and 30 mM *N*′,*N*′-dimethyl-*p*-phenylenediamine (66). Colonies with cbb_3-Cox activity exhibited dark blue staining ($NADI^+$) within 30 s to 1 min, while those with low activity or lacking it showed light blue ($NADI^{slow}$) or no staining ($NADI^-$) up to 15 min, respectively. Total aa_3-Cox and cbb_3-Cox activity levels were determined with reduced cyt *c* as a substrate as done previously (39). Chromatophore membranes were solubilized at room temperature by the addition of 1 mg of DDM/mg of total proteins. Activity assays were initiated by the addition of ~10 μg of solubilized membranes to 1 ml of assay buffer containing 25 μM reduced cyt *c*. Rates of cyt *c* oxidation were determined by monitoring the time-dependent decrease in absorbance at 550 nm and expressed in micromoles of cyt *c* oxidized/min/mg of total membrane proteins by using the extinction coefficient at 550 nm for cyt *c* (ε_{550} = 20.0 mM^{-1} cm^{-1}). The specificity of Cox activity was confirmed by inhibition with 200 μM KCN, a specific inhibitor of HCO enzymes, which stopped cyt *c* oxidation almost completely. Any residual cyanide-insensitive cyt *c* oxidase activity (air oxidation was negligible) was subtracted from the final rates.

Bioinformatic analysis. Genes encoding CcoA-like, CcoN, and Cox1 proteins were identified in the SEED database (45). In addition to amino acid sequence similarity, annotation of a protein as being CcoA-like required conservation of the MXXXM and HXXXM motifs of transmembrane helices 7 and 8. Patterns of co-occurrence and genomic colocalization were detected with the set of tools for comparative genome analysis available in SEED. For the phylogenetic trees of CcoA-like proteins, full-length amino acid sequences (Tables S1, S4, and S5) were aligned through the CIPRES web portal (67) with MAFFT on XSEDE (v. 7.305) (68) and an approximate maximum-likelihood estimation was performed with FastTreeMP on XSEDE (v. 2.1.9) (69). The resulting phylogenetic trees were visualized and annotated with the Interactive Tree of Life (iTOL) tool (70). A comprehensive identification of CcoA homologues in sequenced genomes was performed with a protein similarity network as implemented with the EFI-EST tool (http://efi.igb.illinois.edu/efi-est/) with *R. capsulatus* CcoA as the seed sequence, an E value of 1E-4 for the blast search, and an alignment score of 80. EFI retrieved 2,490 proteins (see Table S4), which were incorporated into the network and visualized with the yFiles organic layout provided with the Cytoscape software (http://www.cytoscape.org).

SUPPLEMENTAL MATERIAL

Supplemental material for this article may be found at https://doi.org/10.1128/mBio.00065-18.

TABLE S1, XLSX file, 0.2 MB.
TABLE S2, DOCX file, 0.01 MB.
TABLE S3, DOCX file, 0.03 MB.
TABLE S4, XLSX file, 0.8 MB.
TABLE S5, XLSX file, 0.2 MB.
TABLE S6, DOCX file, 0.01 MB.

ACKNOWLEDGMENTS

This work was supported mainly by the Division of Chemical Sciences, Geosciences and Biosciences, Office of Basic Energy Sciences of the Department of Energy (DOE DE-FG02-91ER20052 to F.D.), and partly by the National Institutes of Health (NIH GM38237 to F.D.). We acknowledge the partial support provided by the Office of Biological and Environmental Research of the Department of Energy to C.E.B.-H. Support of H.-G.K. by the Deutsche Forschungsgemeinschaft (IRTG 1478 and RTG 2202) is greatly appreciated. The funding agencies had no role in study design, data collection and interpretation, or the decision to submit the work for publication.

We thank Bernd Ludwig for providing the polyclonal antibodies specific for the Cox1 subunit of *P. denitrificans* aa_3-Cox, Shalini Paliwal for help constructing plasmid pSP1, and Stefan Steimle for critical reading of the manuscript.

REFERENCES

1. Öhrvik H, Aaseth J, Horn N. 2017. Orchestration of dynamic copper navigation—new and missing pieces. Metallomics 9:1204–1229. https://doi.org/10.1039/c7mt00010c.
2. Smith AD, Logeman BL, Thiele DJ. 2017. Copper acquisition and utilization in fungi. Annu Rev Microbiol 71:597–623. https://doi.org/10.1146/annurev-micro-030117-020444.
3. Macomber L, Imlay JA. 2009. The iron-sulfur clusters of dehydratases are primary intracellular targets of copper toxicity. Proc Natl Acad Sci U S A 106:8344–8349. https://doi.org/10.1073/pnas.0812808106.
4. Besold AN, Culbertson EM, Culotta VC. 2016. The yin and yang of copper during infection. J Biol Inorg Chem 21:137–144. https://doi.org/10.1007/s00775-016-1335-1.
5. Vulpe C, Levinson B, Whitney S, Packman S, Gitschier J. 1993. Isolation of a candidate gene for Menkes disease and evidence that it encodes a copper-transporting ATPase. Nat Genet 3:7–13. https://doi.org/10.1038/ng0193-7.
6. Tanzi RE, Petrukhin K, Chernov I, Pellequer JL, Wasco W, Ross B, Romano DM, Parano E, Pavone L, Brzustowicz LM, Devoto M, Peppercorn J, Bush AI, Sternlieb I, Honig B, Edelman IS, Soares MB, Scheinberg IH, Gilliam TC 1993. The Wilson disease gene is a copper transporting ATPase with homology to the Menkes disease gene. Nat Genet 5:344–350. https://doi.org/10.1038/ng1293-344.
7. Hung YH, Bush AI, Cherny RA. 2010. Copper in the brain and Alzheimer's disease. J Biol Inorg Chem 15:61–76. https://doi.org/10.1007/s00775-009-0600-y.
8. Baker ZN, Cobine PA, Leary SC. 2017. The mitochondrion: a central architect of copper homeostasis. Metallomics 9:1501–1512. https://doi.org/10.1039/c7mt00221a.
9. Barwinska-Sendra A, Waldron KJ. 2017. The role of intermetal competition and mis-metalation in metal toxicity. Adv Microb Physiol 70:315–379. https://doi.org/10.1016/bs.ampbs.2017.01.003.
10. García-Horsman JA, Barquera B, Rumbley J, Ma J, Gennis RB. 1994. The superfamily of heme-copper respiratory oxidases. J Bacteriol 176:5587–5600. https://doi.org/10.1128/jb.176.18.5587-5600.1994.
11. Timón-Gómez A, Nývltová E, Abriata LA, Vila AJ, Hosler J, Barrientos A. 7 September 2017. Mitochondrial cytochrome *c* oxidase biogenesis: recent developments. Semin Cell Dev Biol https://doi.org/10.1016/j.semcdb.2017.08.055.
12. Pereira MM, Santana M, Teixeira M. 2001. A novel scenario for the evolution of haem-copper oxygen reductases. Biochim Biophys Acta 1505:185–208. https://doi.org/10.1016/S0005-2728(01)00169-4.
13. Michel H, Behr J, Harrenga A, Kannt A. 1998. Cytochrome *c* oxidase: structure and spectroscopy. Annu Rev Biophys Biomol Struct 27:329–356. https://doi.org/10.1146/annurev.biophys.27.1.329.
14. Liu J, Hiser C, Ferguson-Miller S. 2017. Role of conformational change and K-path ligands in controlling cytochrome *c* oxidase activity. Biochem Soc Trans 45:1087–1095. https://doi.org/10.1042/BST20160138.
15. Dancis A, Haile D, Yuan DS, Klausner RD. 1994. The *Saccharomyces cerevisiae* copper transport protein (Ctr1p). Biochemical characterization, regulation by copper, and physiologic role in copper uptake. J Biol Chem 269:25660–25667.
16. Dancis A, Yuan DS, Haile D, Askwith C, Eide D, Moehle C, Kaplan J, Klausner RD. 1994. Molecular characterization of a copper transport protein in *S. cerevisiae*: an unexpected role for copper in iron transport. Cell 76:393–402. https://doi.org/10.1016/0092-8674(94)90345-X.
17. Cobine PA, Ojeda LD, Rigby KM, Winge DR. 2004. Yeast contain a non-proteinaceous pool of copper in the mitochondrial matrix. J Biol Chem 279:14447–14455. https://doi.org/10.1074/jbc.M312693200.
18. Horng YC, Cobine PA, Maxfield AB, Carr HS, Winge DR. 2004. Specific copper transfer from the Cox17 metallochaperone to both Sco1 and Cox11 in the assembly of yeast cytochrome *c* oxidase. J Biol Chem 279:35334–35340. https://doi.org/10.1074/jbc.M404747200.
19. Leary SC, Kaufman BA, Pellecchia G, Guercin GH, Mattman A, Jaksch M, Shoubridge EA. 2004. Human SCO1 and SCO2 have independent, cooperative functions in copper delivery to cytochrome *c* oxidase. Hum Mol Genet 13:1839–1848. https://doi.org/10.1093/hmg/ddh197.
20. Carr HS, George GN, Winge DR. 2002. Yeast Cox11, a protein essential for cytochrome *c* oxidase assembly, is a Cu(I)-binding protein. J Biol Chem 277:31237–31242. https://doi.org/10.1074/jbc.M204854200.
21. Baker ZN, Jett K, Boulet A, Hossain A, Cobine PA, Kim BE, El Zawily AM, Lee L, Tibbits GF, Petris MJ, Leary SC. 2017. The mitochondrial metallochaperone SCO1 maintains CTR1 at the plasma membrane to preserve copper homeostasis in the murine heart. Hum Mol Genet 26:4617–4628. https://doi.org/10.1093/hmg/ddx344.
22. Banci L, Bertini I, Ciofi-Baffoni S, Katsari E, Katsaros N, Kubicek K, Mangani S. 2005. A copper(I) protein possibly involved in the assembly of Cu_A center of bacterial cytochrome *c* oxidase. Proc Natl Acad Sci U S A 102:3994–3999. https://doi.org/10.1073/pnas.0406150102.
23. Swem DL, Swem LR, Setterdahl A, Bauer CE. 2005. Involvement of SenC in assembly of cytochrome *c* oxidase in *Rhodobacter capsulatus*. J Bacteriol 187:8081–8087. https://doi.org/10.1128/JB.187.23.8081-8087.2005.

24. Thompson AK, Gray J, Liu A, Hosler JP. 2012. The roles of *Rhodobacter sphaeroides* copper chaperones PCu_AC and Sco (PrrC) in the assembly of the copper centers of the aa_3-type and the cbb_3-type cytochrome *c* oxidases. Biochim Biophys Acta 1817:955–964. https://doi.org/10.1016/j.bbabio.2012.01.003.
25. Hiser L, Di Valentin M, Hamer AG, Hosler JP. 2000. Cox11p is required for stable formation of the Cu_B and magnesium centers of cytochrome *c* oxidase. J Biol Chem 275:619–623. https://doi.org/10.1074/jbc.275.1.619.
26. Ducluzeau AL, Ouchane S, Nitschke W. 2008. The cbb_3 oxidases are an ancient innovation of the domain bacteria. Mol Biol Evol 25:1158–1166. https://doi.org/10.1093/molbev/msn062.
27. Ekici S, Pawlik G, Lohmeyer E, Koch HG, Daldal F. 2012. Biogenesis of cbb_3-type cytochrome *c* oxidase in *Rhodobacter capsulatus*. Biochim Biophys Acta 1817:898–910. https://doi.org/10.1016/j.bbabio.2011.10.011.
28. Buschmann S, Warkentin E, Xie H, Langer JD, Ermler U, Michel H. 2010. The structure of cbb_3 cytochrome oxidase provides insights into proton pumping. Science 329:327–330. https://doi.org/10.1126/science.1187303.
29. Koch HG, Winterstein C, Saribas AS, Alben JO, Daldal F. 2000. Roles of the ccoGHIS gene products in the biogenesis of the cbb_3-type cytochrome *c* oxidase. J Mol Biol 297:49–65. https://doi.org/10.1006/jmbi.2000.3555.
30. González-Guerrero M, Raimunda D, Cheng X, Argüello JM. 2010. Distinct functional roles of homologous Cu^+ efflux ATPases in *Pseudomonas aeruginosa*. Mol Microbiol 78:1246–1258. https://doi.org/10.1111/j.1365-2958.2010.07402.x.
31. Hassani BK, Astier C, Nitschke W, Ouchane S. 2010. CtpA, a copper-translocating P-type ATPase involved in the biogenesis of multiple copper-requiring enzymes. J Biol Chem 285:19330–19337. https://doi.org/10.1074/jbc.M110.116020.
32. Ekici S, Turkarslan S, Pawlik G, Dancis A, Baliga NS, Koch HG, Daldal F. 2014. Intracytoplasmic copper homeostasis controls cytochrome *c* oxidase production. mBio 5:e01055-13. https://doi.org/10.1128/mBio.01055-13.
33. Trasnea PI, Utz M, Khalfaoui-Hassani B, Lagies S, Daldal F, Koch HG. 2016. Cooperation between two periplasmic copper chaperones is required for full activity of the cbb_3 -type cytochrome *c* oxidase and copper homeostasis in *Rhodobacter capsulatus*. Mol Microbiol 100:345–361. https://doi.org/10.1111/mmi.13321.
34. Ekici S, Yang H, Koch HG, Daldal F. 2012. Novel transporter required for biogenesis of cbb_3-type cytochrome *c* oxidase in *Rhodobacter capsulatus*. mBio 3:e00293-11. https://doi.org/10.1128/mBio.00293-11.
35. Beaudoin J, Ekici S, Daldal F, Ait-Mohand S, Guérin B, Labbé S. 2013. Copper transport and regulation in *Schizosaccharomyces pombe*. Biochem Soc Trans 41:1679–1686. https://doi.org/10.1042/BST2013089.
36. Saier MH, Jr., Reddy VS, Tsu BV, Ahmed MS, Li C, Moreno-Hagelsieb G. 2016. The Transporter Classification Database (TCDB): recent advances. Nucleic Acids Res 44:D372–D379. https://doi.org/10.1093/nar/gkv1103.
37. Khalfaoui-Hassani B, Verissimo AF, Koch HG, Daldal F. 2016. Uncovering the transmembrane metal binding site of the novel bacterial major facilitator superfamily-type copper importer CcoA. mBio 7:e01981-15. https://doi.org/10.1128/mBio.01981-15.
38. Shapleigh JP, Gennis RB. 1992. Cloning, sequencing and deletion from the chromosome of the gene encoding subunit I of the aa_3-type cytochrome *c* oxidase of *Rhodobacter sphaeroides*. Mol Microbiol 6:635–642. https://doi.org/10.1111/j.1365-2958.1992.tb01511.x.
39. Daldal F, Mandaci S, Winterstein C, Myllykallio H, Duyck K, Zannoni D. 2001. Mobile cytochrome c_2 and membrane-anchored cytochrome c_y are both efficient electron donors to the cbb_3- and aa_3-type cytochrome *c* oxidases during respiratory growth of *Rhodobacter sphaeroides*. J Bacteriol 183:2013–2024. https://doi.org/10.1128/JB.183.6.2013-2024.2001.
40. Toledo-Cuevas M, Barquera B, Gennis RB, Wikström M, García-Horsman JA. 1998. The cbb_3-type cytochrome *c* oxidase from *Rhodobacter sphaeroides*, a proton-pumping heme-copper oxidase. Biochim Biophys Acta 1365:421–434. https://doi.org/10.1016/S0005-2728(98)00095-4.
41. Hosler JP, Fetter J, Tecklenburg MM, Espe M, Lerma C, Ferguson-Miller S. 1992. Cytochrome aa_3 of *Rhodobacter sphaeroides* as a model for mitochondrial cytochrome *c* oxidase. Purification, kinetics, proton pumping, and spectral analysis. J Biol Chem 267:24264–24272.
42. Thomas PE, Ryan D, Levin W. 1976. Improved staining procedure for detection of peroxidase activity of cytochrome P-450 on sodium dodecyl-sulfate polyacrylamide gels. Anal Biochem 75:168–176. https://doi.org/10.1016/0003-2697(76)90067-1.
43. Gurumoorthy P, Ludwig B. 2015. Deciphering protein-protein interactions during the biogenesis of cytochrome *c* oxidase from *Paracoccus denitrificans*. FEBS J 282:537–549. https://doi.org/10.1111/febs.13160.
44. Peuser V, Glaeser J, Klug G. 2011. The RSP_2889 gene product of *Rhodobacter sphaeroides* is a CueR homologue controlling copper-responsive genes. Microbiology 157:3306–3313. https://doi.org/10.1099/mic.0.051607-0.
45. Overbeek R, Begley T, Butler RM, Choudhuri JV, Chuang HY, Cohoon M, de Crécy-Lagard V, Diaz N, Disz T, Edwards R, Fonstein M, Frank ED, Gerdes S, Glass EM, Goesmann A, Hanson A, Iwata-Reuyl D, Jensen R, Jamshidi N, Krause L, Kubal M, Larsen N, Linke B, McHardy AC, Meyer F, Neuweger H, Olsen G, Olson R, Osterman A, Portnoy V, Pusch GD, Rodionov DA, Rückert C, Steiner J, Stevens R, Thiele I, Vassieva O, Ye Y, Zagnitko O, Vonstein V. 2005. The subsystems approach to genome annotation and its use in the project to annotate 1000 genomes. Nucleic Acids Res 33:5691–5702. https://doi.org/10.1093/nar/gki866.
46. Ekici S, Jiang X, Koch HG, Daldal F. 2013. Missense mutations in cytochrome *c* maturation genes provide new insights into *Rhodobacter capsulatus* cbb_3-type cytochrome *c* oxidase biogenesis. J Bacteriol 195:261–269. https://doi.org/10.1128/JB.01415-12.
47. Schimo S, Wittig I, Pos KM, Ludwig B. 2017. Cytochrome *c* oxidase biogenesis and metallochaperone interactions: steps in the assembly pathway of a bacterial complex. PLoS One 12:e0170037. https://doi.org/10.1371/journal.pone.0170037.
48. Sandri F, Fedi S, Cappelletti M, Calabrese FM, Turner RJ, Zannoni D. 2017. Biphenyl modulates the expression and function of respiratory oxidases in the polychlorinated-biphenyls degrader *Pseudomonas pseudoalcaligenes* KF707. Front Microbiol 8:1223. https://doi.org/10.3389/fmicb.2017.01223.
49. Pereira MM, Sousa FL, Veríssimo AF, Teixeira M. 2008. Looking for the minimum common denominator in haem-copper oxygen reductases: towards a unified catalytic mechanism. Biochim Biophys Acta 1777:929–934. https://doi.org/10.1016/j.bbabio.2008.05.441.
50. Rae TD, Schmidt PJ, Pufahl RA, Culotta VC, O'Halloran TV. 1999. Undetectable intracellular free copper: the requirement of a copper chaperone for superoxide dismutase. Science 284:805–808. https://doi.org/10.1126/science.284.5415.805.
51. O'Halloran TV, Culotta VC. 2000. Metallochaperones, an intracellular shuttle service for metal ions. J Biol Chem 275:25057–25060. https://doi.org/10.1074/jbc.R000006200.
52. Glerum DM, Shtanko A, Tzagoloff A. 1996. SCO1 and SCO2 act as high copy suppressors of a mitochondrial copper recruitment defect in *Saccharomyces cerevisiae*. J Biol Chem 271:20531–20535. https://doi.org/10.1074/jbc.271.34.20531.
53. Lovett ST. 2004. Encoded errors: mutations and rearrangements mediated by misalignment at repetitive DNA sequences. Mol Microbiol 52:1243–1253. https://doi.org/10.1111/j.1365-2958.2004.04076.x.
54. Moxon R, Bayliss C, Hood D. 2006. Bacterial contingency loci: the role of simple sequence DNA repeats in bacterial adaptation. Annu Rev Genet 40:307–333. https://doi.org/10.1146/annurev.genet.40.110405.090442.
55. Zhou K, Aertsen A, Michiels CW. 2014. The role of variable DNA tandem repeats in bacterial adaptation. FEMS Microbiol Rev 38:119–141. https://doi.org/10.1111/1574-6976.12036.
56. Lin WH, Kussell E. 2012. Evolutionary pressures on simple sequence repeats in prokaryotic coding regions. Nucleic Acids Res 40:2399–2413. https://doi.org/10.1093/nar/gkr1078.
57. Gourdon P, Liu XY, Skjørringe T, Morth JP, Møller LB, Pedersen BP, Nissen P. 2011. Crystal structure of a copper-transporting P_{IB}-type ATPase. Nature 475:59–64. https://doi.org/10.1038/nature10191.
58. Fu Y, Tsui HC, Bruce KE, Sham LT, Higgins KA, Lisher JP, Kazmierczak KM, Maroney MJ, Dann CE III, Winkler ME, Giedroc DP. 2013. A new structural paradigm in copper resistance in *Streptococcus pneumoniae*. Nat Chem Biol 9:177–183. https://doi.org/10.1038/nchembio.1168.
59. Blaby-Haas CE, Padilla-Benavides T, Stübe R, Argüello JM, Merchant SS. 2014. Evolution of a plant-specific copper chaperone family for chloroplast copper homeostasis. Proc Natl Acad Sci U S A 111:E5480–E5487. https://doi.org/10.1073/pnas.1421545111.
60. Drees SL, Beyer DF, Lenders-Lomscher C, Lübben M. 2015. Distinct functions of serial metal-binding domains in the *Escherichia coli* P1 B-ATPase CopA. Mol Microbiol 97:423–438. https://doi.org/10.1111/mmi.13038.
61. Meydan S, Klepacki D, Karthikeyan S, Margus T, Thomas P, Jones JE, Khan Y, Briggs J, Dinman JD, Vázquez-Laslop N, Mankin AS. 2017. Programmed ribosomal frameshifting generates a copper transporter and a copper chaperone from the same gene. Mol Cell 65:207–219. https://doi.org/10.1016/j.molcel.2016.12.008.
62. Ettema TJ, Huynen MA, de Vos WM, van der Oost J. 2003. TRASH: a novel

metal-binding domain predicted to be involved in heavy-metal sensing, trafficking and resistance. Trends Biochem Sci 28:170–173. https://doi.org/10.1016/S0968-0004(03)00037-9.
63. Sambrook J, Russell DW. 2001. Molecular cloning: a laboratory manual, 3rd ed. Cold Spring Harbor Laboratory Press, Cold Spring Harbor, NY.
64. Sistrom WR. 1960. A requirement for sodium in the growth of *Rhodopseudomonas spheroides*. J Gen Microbiol 22:778–785. https://doi.org/10.1099/00221287-22-3-778.
65. Gray KA, Davidson E, Daldal F. 1992. Mutagenesis of methionine-183 drastically affects the physicochemical properties of cytochrome c_1 of the bc_1 complex of *Rhodobacter capsulatus*. Biochemistry 31:11864–11873. https://doi.org/10.1021/bi00162a027.
66. Marrs B, Stahl CL, Lien S, Gest H. 1972. Biochemical physiology of a respiration-deficient mutant of the photosynthetic bacterium *Rhodopseudomonas capsulata*. Proc Natl Acad Sci U S A 69:916–920.
67. Miller MA, Pfeiffer W, Schwartz T. 2010. Creating the CIPRES Science Gateway for inference of large phylogenetic trees, p 45–52. *In*. Proceedings of the Gateway Computing Environments Workshop (GCE 2010), New Orleans, LA, 14 November 2010. Institute of Electrical and Electronics Engineers, Piscataway, NJ. http://www.phylo.org/sub_sections/portal/sc2010_paper.pdf.
68. Katoh K, Standley DM. 2013. MAFFT multiple sequence alignment software version 7: improvements in performance and usability. Mol Biol Evol 30:772–780. https://doi.org/10.1093/molbev/mst010.
69. Price MN, Dehal PS, Arkin AP. 2010. FastTree 2—approximately maximum-likelihood trees for large alignments. PLoS One 5:e9490. https://doi.org/10.1371/journal.pone.0009490.
70. Letunic I, Bork P. 2016. Interactive tree of life (iTOL) v3: an online tool for the display and annotation of phylogenetic and other trees. Nucleic Acids Res 44:W242–W245. https://doi.org/10.1093/nar/gkw290.
71. Boulet A, Vest KE, Maynard MK, Gammon MG, Russell AC, Mathews AT, Cole SE, Zhu X, Phillips CB, Kwong JQ, Dodani SC, Leary SC, Cobine PA. 13 December 2017. The mammalian phosphate carrier SLC25A3 is a mitochondrial copper transporter required for cytochrome *c* oxidase biogenesis. J Biol Chem https://doi.org/10.1074/jbc.RA117.000265.